

All-sky LIGO Search for Periodic Gravitational Waves in the Early S5 Data

- B. Abbott,¹⁶ R. Abbott,¹⁶ R. Adhikari,¹⁶ P. Ajith,² B. Allen,^{2, 54} G. Allen,³² R. Amin,²⁰ S. B. Anderson,¹⁶ W. G. Anderson,⁵⁴ M. A. Arain,⁴¹ M. Araya,¹⁶ H. Armandula,¹⁶ P. Armor,⁵⁴ Y. Aso,¹⁰ S. Aston,⁴⁰ P. Aufmuth,¹⁵ C. Aubert,² S. Babak,¹ S. Ballmer,¹⁶ H. Bantilan,⁸ B. C. Barish,¹⁶ C. Barker,¹⁸ D. Barker,¹⁸ B. Barr,⁴² P. Barriga,⁵³ M. A. Barton,⁴² M. Bastarrika,⁴² K. Bayer,¹⁷ J. Betzwieser,¹⁶ P. T. Beyersdorf,²⁸ I. A. Bilenko,²³ G. Billingsley,¹⁶ R. Biswas,⁵⁴ E. Black,¹⁶ K. Blackburn,¹⁶ L. Blackburn,¹⁷ D. Blair,⁵³ B. Bland,¹⁸ T. P. Bodiya,¹⁷ L. Bogue,¹⁹ R. Bork,¹⁶ V. Boschi,¹⁶ S. Bose,⁵⁵ P. R. Brady,⁵⁴ V. B. Braginsky,²³ J. E. Brau,⁴⁷ M. Brinkmann,² A. Brooks,¹⁶ D. A. Brown,³³ G. Brunet,¹⁷ A. Bullington,³² A. Buonanno,⁴³ O. Burmeister,² R. L. Byer,³² L. Cadonati,⁴⁴ G. Cagnoli,⁴² J. B. Camp,²⁴ J. Cannizzo,²⁴ K. Cannon,¹⁶ J. Cao,¹⁷ L. Cardenas,¹⁶ S. Caride,⁸ T. Casebolt,³² G. Castaldi,⁵⁰ C. Cepeda,¹⁶ E. Chalkley,⁴² P. Charlton,⁹ S. Chatterji,¹⁶ S. Chelkowski,⁴⁰ Y. Chen,^{6, 1} N. Christensen,⁸ D. Clark,³² J. Clark,⁴² T. Cokelaer,⁷ R. Conte,⁴⁹ D. Cook,¹⁸ T. Corbitt,¹⁷ D. Coyne,¹⁶ J. D. E. Creighton,⁵⁴ A. Cumming,⁴² L. Cunningham,⁴² R. M. Cutler,⁴⁰ J. Dalrymple,³³ K. Danzmann,^{15, 2} G. Davies,⁷ D. DeBra,³² J. Degallaix,¹ M. Degree,³² V. Dergachev,⁴⁵ S. Desai,³⁴ R. DeSalvo,¹⁶ S. Dhurandhar,¹⁴ M. Díaz,³⁶ J. Dickson,⁴ A. Dietz,⁷ F. Donovan,¹⁷ K. L. Dooley,⁴¹ E. E. Doomes,³¹ R. W. P. Drever,⁵ I. Duke,¹⁷ J.-C. Dumas,⁵³ R. J. Dupuis,¹⁶ J. G. Dwyer,¹⁰ C. Echols,¹⁶ A. Effler,¹⁸ P. Ehrens,¹⁶ G. Ely,⁸ E. Espinoza,¹⁶ T. Etzel,¹⁶ T. Evans,¹⁹ S. Fairhurst,⁷ Y. Fan,⁵³ D. Fazi,¹⁶ H. Fehrmann,² M. M. Fejer,³² L. S. Finn,³⁴ K. Flasch,⁵⁴ N. Fotopoulos,⁵⁴ A. Freise,⁴⁰ R. Frey,⁴⁷ T. Fricke,^{16, 48} P. Fritschel,¹⁷ V. V. Frolov,¹⁹ M. Fyffe,¹⁹ J. Garofoli,¹⁸ I. Gholami,¹ J. A. Giaime,^{19, 20} S. Giampanis,⁴⁸ K. D. Giardina,¹⁹ K. Goda,¹⁷ E. Goetz,⁴⁵ L. Goggin,¹⁶ G. González,²⁰ S. Gossler,² R. Gouaty,²⁰ A. Grant,⁴² S. Gras,⁵³ C. Gray,¹⁸ M. Gray,⁴ R. J. S. Greenhalgh,²⁷ A. M. Gretarsson,¹¹ F. Grimaldi,¹⁷ R. Grosso,³⁶ H. Grote,² S. Grunewald,¹ M. Guenther,¹⁸ E. K. Gustafson,¹⁶ R. Gustafson,⁴⁵ B. Hage,¹⁵ J. M. Hallam,⁴⁰ D. Hammer,⁵⁴ C. Hanna,²⁰ J. Hanson,¹⁹ J. Harms,² G. Harry,¹⁷ E. Harstad,⁴⁷ K. Hayama,³⁶ T. Hayler,²⁷ J. Heefner,¹⁶ I. S. Heng,⁴² M. Hennessy,³² A. Heptonstall,⁴² M. Hewitson,² S. Hild,⁴⁰ E. Hirose,³³ D. Hoak,¹⁹ D. Hosken,³⁹ J. Hough,⁴² S. H. Huttner,⁴² D. Ingram,¹⁸ M. Ito,⁴⁷ A. Ivanov,¹⁶ B. Johnson,¹⁸ W. W. Johnson,²⁰ D. I. Jones,⁵¹ G. Jones,⁷ R. Jones,⁴² L. Ju,⁵³ P. Kalmus,¹⁰ V. Kalogera,²⁶ S. Kamat,¹⁰ J. Kanner,⁴³ D. Kasprzyk,⁴⁰ E. Katsavounidis,¹⁷ K. Kawabe,¹⁸ S. Kawamura,²⁵ F. Kawazoe,²⁵ W. Kells,¹⁶ D. G. Keppel,¹⁶ F. Ya. Khalili,²³ R. Khan,¹⁰ E. Khazanov,¹³ C. Kim,²⁶ P. King,¹⁶ J. S. Kissel,²⁰ S. Klimenko,⁴¹ K. Kokeyama,²⁵ V. Kondrashov,¹⁶ R. K. Kopparapu,³⁴ D. Kozak,¹⁶ I. Kozhevnikov,¹³ B. Krishnan,¹ P. Kwee,¹⁵ P. K. Lam,⁴ M. Landry,¹⁸ M. M. Lang,³⁴ B. Lantz,³² A. Lazzarini,¹⁶ M. Lei,¹⁶ N. Leindegger,³² V. Leonhardt,²⁵ I. Leonor,⁴⁷ K. Libbrecht,¹⁶ H. Lin,⁴¹ P. Lindquist,¹⁶ N. A. Lockerbie,⁵² D. Lodhia,⁴⁰ M. Lormand,¹⁹ P. Lu,³² M. Lubinski,¹⁸ A. Lucianetti,⁴¹ H. Lück,^{15, 2} B. Machenschalk,² M. MacInnis,¹⁷ M. Mageswaran,¹⁶ K. Mailand,¹⁶ V. Mandic,⁴⁶ S. Márka,¹⁰ Z. Márka,¹⁰ A. Markosyan,³² J. Markowitz,¹⁷ E. Maros,¹⁶ I. Martin,⁴² R. M. Martin,⁴¹ J. N. Marx,¹⁶ K. Mason,¹⁷ F. Matichard,²⁰ L. Matone,¹⁰ R. Matzner,³⁵ N. Mavalvala,¹⁷ R. McCarthy,¹⁸ D. E. McClelland,⁴ S. C. McGuire,³¹ M. McHugh,²² G. McIntyre,¹⁶ G. McIvor,³⁵ D. McKechan,⁷ K. McKenzie,⁴ T. Meier,¹⁵ A. Melissinos,⁴⁸ G. Mendell,¹⁸ R. A. Mercer,⁴¹ S. Meshkov,¹⁶ C. J. Messenger,² D. Meyers,¹⁶ J. Miller,^{42, 16} J. Minelli,³⁴ S. Mitra,¹⁴ V. P. Mitrofanov,²³ G. Mitselmakher,⁴¹ R. Mittleman,¹⁷ O. Miyakawa,¹⁶ B. Moe,⁵⁴ S. Mohanty,³⁶ G. Moreno,¹⁸ K. Mossavi,² C. MowLowry,⁴ G. Mueller,⁴¹ S. Mukherjee,³⁶ H. Mukhopadhyay,¹⁴ H. Müller-Ebhardt,² J. Munch,³⁹ P. Murray,⁴² E. Myers,¹⁸ J. Myers,¹⁸ T. Nash,¹⁶ J. Nelson,⁴² G. Newton,⁴² A. Nishizawa,²⁵ K. Numata,²⁴ J. O'Dell,²⁷ G. Ogin,¹⁶ B. O'Reilly,¹⁹ R. O'Shaughnessy,³⁴ D. J. Ottaway,¹⁷ R. S. Ottens,⁴¹ H. Overmier,¹⁹ B. J. Owen,³⁴ Y. Pan,⁴³ C. Pankow,⁴¹ M. A. Papa,^{1, 54} V. Parameshwaraiah,¹⁸ P. Patel,¹⁶ M. Pedraza,¹⁶ S. Penn,¹² A. Perreca,⁴⁰ T. Petrie,³⁴ I. M. Pinto,⁵⁰ M. Pitkin,⁴² H. J. Pletsch,² M. V. Plissi,⁴² F. Postiglione,⁴⁹ M. Principe,⁵⁰ R. Prix,² V. Quetschke,⁴¹ F. Raab,¹⁸ D. S. Rabeling,⁴ H. Radkins,¹⁸ N. Rainer,² M. Rakhmanov,³⁰ M. Ramsunder,³⁴ H. Rehbein,² S. Reid,⁴² D. H. Reitze,⁴¹ R. Riesen,¹⁹ K. Riles,⁴⁵ B. Rivera,¹⁸ N. A. Robertson,^{16, 42} C. Robinson,⁷ E. L. Robinson,⁴⁰ S. Roddy,¹⁹ A. Rodriguez,²⁰ A. M. Rogan,⁵⁵ J. Rollins,¹⁰ J. D. Romano,³⁶ J. Romie,¹⁹ R. Route,³² S. Rowan,⁴² A. Rüdiger,² L. Ruet,¹⁷ P. Russell,¹⁶ K. Ryan,¹⁸ S. Sakata,²⁵ M. Samidi,¹⁶ L. Sancho de la Jordana,³⁸ V. Sandberg,¹⁸ V. Sannibale,¹⁶ S. Saraf,²⁹ P. Sarin,¹⁷ B. S. Sathyaprakash,⁷ S. Sato,²⁵ P. R. Saulson,³³ R. Savage,¹⁸ P. Savov,⁶ S. W. Schediwy,⁵³ R. Schilling,² R. Schnabel,² R. Schofield,⁴⁷ B. F. Schutz,^{1, 7} P. Schwinberg,¹⁸ S. M. Scott,⁴ A. C. Searle,⁴ B. Sears,¹⁶ F. Seifert,² D. Sellers,¹⁹ A. S. Sengupta,¹⁶ P. Shawhan,⁴³ D. H. Shoemaker,¹⁷ A. Sibley,¹⁹ X. Siemens,⁵⁴ D. Sigg,¹⁸ S. Sinha,³² A. M. Sintes,^{38, 1} B. J. J. Slagmolen,⁴ J. Slutsky,²⁰ J. R. Smith,³³ M. R. Smith,¹⁶ N. D. Smith,¹⁷ K. Somiya,^{2, 1} B. Sorazu,⁴² L. C. Stein,¹⁷ A. Stochino,¹⁶ R. Stone,³⁶ K. A. Strain,⁴² D. M. Strom,⁴⁷ A. Stuver,¹⁹ T. Z. Summerscales,³ K.-X. Sun,³² M. Sung,²⁰ P. J. Sutton,⁷ H. Takahashi,¹ D. B. Tanner,⁴¹ R. Taylor,¹⁶ R. Taylor,⁴² J. Thacker,¹⁹ K. A. Thorne,³⁴ K. S. Thorne,⁶ A. Thüring,¹⁵ K. V. Tokmakov,⁴²

C. Torres,¹⁹ C. Torrie,⁴² G. Traylor,¹⁹ M. Trias,³⁸ W. Tyler,¹⁶ D. Ugolini,³⁷ J. Ulmen,³² K. Urbanek,³² H. Vahlbruch,¹⁵ C. Van Den Broeck,⁷ M. van der Sluys,²⁶ S. Vass,¹⁶ R. Vaulin,⁵⁴ A. Vecchio,⁴⁰ J. Veitch,⁴⁰ P. Veitch,³⁹ A. Villar,¹⁶ C. Vorvick,¹⁸ S. P. Vyachanin,²³ S. J. Waldman,¹⁶ L. Wallace,¹⁶ H. Ward,⁴² R. Ward,¹⁶ M. Weinert,² A. Weinstein,¹⁶ R. Weiss,¹⁷ S. Wen,²⁰ K. Wette,⁴ J. T. Whelan,¹ S. E. Whitcomb,¹⁶ B. F. Whiting,⁴¹ C. Wilkinson,¹⁸ P. A. Willems,¹⁶ H. R. Williams,³⁴ L. Williams,⁴¹ B. Willke,^{15,2} I. Wilmot,²⁷ W. Winkler,² C. C. Wipf,¹⁷ A. G. Wiseman,⁵⁴ G. Woan,⁴² R. Wooley,¹⁹ J. Worden,¹⁸ W. Wu,⁴¹ I. Yakushin,¹⁹ H. Yamamoto,¹⁶ Z. Yan,⁵³ S. Yoshida,³⁰ M. Zanolin,¹¹ J. Zhang,⁴⁵ L. Zhang,¹⁶ C. Zhao,⁵³ N. Zotov,²¹ M. Zucker,¹⁷ and J. Zweizig¹⁶

(The LIGO Scientific Collaboration, <http://www.ligo.org>)

¹Albert-Einstein-Institut, Max-Planck-Institut für Gravitationsphysik, D-14476 Golm, Germany

²Albert-Einstein-Institut, Max-Planck-Institut für Gravitationsphysik, D-30167 Hannover, Germany

³Andrews University, Berrien Springs, MI 49104 USA

⁴Australian National University, Canberra, 0200, Australia

⁵California Institute of Technology, Pasadena, CA 91125, USA

⁶Caltech-CaRT, Pasadena, CA 91125, USA

⁷Cardiff University, Cardiff, CF24 3AA, United Kingdom

⁸Carleton College, Northfield, MN 55057, USA

⁹Charles Sturt University, Wagga Wagga, NSW 2678, Australia

¹⁰Columbia University, New York, NY 10027, USA

¹¹Embry-Riddle Aeronautical University, Prescott, AZ 86301 USA

¹²Hobart and William Smith Colleges, Geneva, NY 14456, USA

¹³Institute of Applied Physics, Nizhny Novgorod, 603950, Russia

¹⁴Inter-University Centre for Astronomy and Astrophysics, Pune - 411007, India

¹⁵Leibniz Universität Hannover, D-30167 Hannover, Germany

¹⁶LIGO - California Institute of Technology, Pasadena, CA 91125, USA

¹⁷LIGO - Massachusetts Institute of Technology, Cambridge, MA 02139, USA

¹⁸LIGO Hanford Observatory, Richland, WA 99352, USA

¹⁹LIGO Livingston Observatory, Livingston, LA 70754, USA

²⁰Louisiana State University, Baton Rouge, LA 70803, USA

²¹Louisiana Tech University, Ruston, LA 71272, USA

²²Loyola University, New Orleans, LA 70118, USA

²³Moscow State University, Moscow, 119992, Russia

²⁴NASA/Goddard Space Flight Center, Greenbelt, MD 20771, USA

²⁵National Astronomical Observatory of Japan, Tokyo 181-8588, Japan

²⁶Northwestern University, Evanston, IL 60208, USA

²⁷Rutherford Appleton Laboratory, Chilton, Didcot, Oxon OX11 0QX United Kingdom

²⁸San Jose State University, San Jose, CA 95192, USA

²⁹Sonoma State University, Rohnert Park, CA 94928, USA

³⁰Southeastern Louisiana University, Hammond, LA 70402, USA

³¹Southern University and A&M College, Baton Rouge, LA 70813, USA

³²Stanford University, Stanford, CA 94305, USA

³³Syracuse University, Syracuse, NY 13244, USA

³⁴The Pennsylvania State University, University Park, PA 16802, USA

³⁵The University of Texas at Austin, Austin, TX 78712, USA

³⁶The University of Texas at Brownsville and Texas Southmost College, Brownsville, TX 78520, USA

³⁷Trinity University, San Antonio, TX 78212, USA

³⁸Universitat de les Illes Balears, E-07122 Palma de Mallorca, Spain

³⁹University of Adelaide, Adelaide, SA 5005, Australia

⁴⁰University of Birmingham, Birmingham, B15 2TT, United Kingdom

⁴¹University of Florida, Gainesville, FL 32611, USA

⁴²University of Glasgow, Glasgow, G12 8QQ, United Kingdom

⁴³University of Maryland, College Park, MD 20742 USA

⁴⁴University of Massachusetts, Amherst, MA 01003 USA

⁴⁵University of Michigan, Ann Arbor, MI 48109, USA

⁴⁶University of Minnesota, Minneapolis, MN 55455, USA

⁴⁷University of Oregon, Eugene, OR 97403, USA

⁴⁸University of Rochester, Rochester, NY 14627, USA

⁴⁹University of Salerno, 84084 Fisciano (Salerno), Italy

⁵⁰University of Sannio at Benevento, I-82100 Benevento, Italy

⁵¹University of Southampton, Southampton, SO17 1BJ, United Kingdom

⁵²University of Strathclyde, Glasgow, G1 1XQ, United Kingdom

⁵³University of Western Australia, Crawley, WA 6009, Australia

⁵⁴University of Wisconsin-Milwaukee, Milwaukee, WI 53201, USA

We report on an all-sky search with the LIGO detectors for periodic gravitational waves in the frequency range 50–1100 Hz and with the frequency’s time derivative in the range -5×10^{-9} – 0 Hz s^{-1} . Data from the first eight months of the fifth LIGO science run (S5) have been used in this search, which is based on a semi-coherent method (PowerFlux) of summing strain power. Observing no evidence of periodic gravitational radiation, we report 95% confidence-level upper limits on radiation emitted by any unknown isolated rotating neutron stars within the search range. Strain limits below 10^{-24} are obtained over a 200-Hz band, and the sensitivity improvement over previous searches increases the spatial volume sampled by an average factor of about 100 over the entire search band. For a neutron star with nominal equatorial ellipticity of 10^{-6} , the search is sensitive to distances as great as 500 pc—a range that could encompass many undiscovered neutron stars, albeit only a tiny fraction of which would likely be rotating fast enough to be accessible to LIGO. This ellipticity is at the upper range thought to be sustainable by conventional neutron stars and well below the maximum sustainable by a strange quark star.

PACS numbers: 04.80.Nn, 95.55.Ym, 97.60.Gb, 07.05.Kf

I. INTRODUCTION

We have carried out an all-sky search with the LIGO (Laser Interferometer Gravitational-wave Observatory) detectors [1, 2] for periodic gravitational waves, using data from the first eight months of LIGO’s fifth science run (S5). We have searched over the frequency range 50–1100 Hz, allowing for a frequency time derivative in the range -5×10^{-9} – 0 Hz s^{-1} . Rotating neutron stars in our galaxy are the prime target. At signal frequencies near 100 Hz we obtain strain sensitivities below 10^{-24} , a strain at which one might optimistically expect to see the strongest signal from a previously unknown neutron star according to a generic argument originally made by Blandford (unpublished), and extended in our previous search for such objects in S2 data [3]. A recent refinement of the argument [4] gives less optimistic estimates, but these too are surpassed by the experimental results presented here.

Using data from earlier science runs, the LIGO Scientific Collaboration (LSC) has previously reported on all-sky searches for unknown rotating neutron stars (henceforth designated as “pulsars” here). These searches have been performed using a short-period coherent search in the 160.0–728.8 Hz frequency range [3], and using a long-period semi-coherent search in the 200–400 Hz frequency range in the S2 data [5] and the 50–1000 Hz range in the S4 data [6]. Einstein@Home, a distributed home computing effort [7], has also been running searches using a coherent first stage, followed by a simple coincidence stage, for which S3 and S4 results have been released [8, 9].

The data collected in the S5 data run were more sensitive than in previous data runs, and the amount of data used here is an increase by a factor of eight over that reported from the S4 data run [6], resulting in upper limits on periodic gravitational waves about a factor of 3–6 lower than those from the S4 data, depending on source frequency. This improvement gives an increase in sampled galactic volume by about a factor of 100, depending on the assumed source frequency and spin-down.

At a signal frequency of 1100 Hz we achieve sensitivity to neutron stars of equatorial ellipticity $\epsilon \sim 10^{-6}$ at distances up to 500 pc (see [6] for relations). This ellipticity is at the upper range thought to be sustainable by conventional neutron stars [10] and well below the maximum sustainable (10^{-4}) by a strange quark star [11]. The number of undiscovered, electromagnetically quiet neutron stars within 500 pc can be estimated to be $O(10^4 - 10^5)$ from the neutron star birth rate [12], although it is likely that only a tiny fraction would both be rotating fast enough to be accessible to LIGO [13] and remain in the local volume over the age of the galaxy [14]. Only ~ 25 radio or x-ray pulsars have been discovered so far within that volume [15].

II. THE LIGO DETECTORS AND THE S5 SCIENCE RUN

The LIGO detector network consists of a 4-km interferometer in Livingston Louisiana, (L1), and two interferometers in Hanford Washington, one 4-km and the other 2-km (H1 and H2).

The data analyzed in this paper were produced in the first eight months of LIGO’s fifth science run (S5). This run started at 16:00 UTC on November 4, 2005 at the LIGO Hanford Observatory and at 16:00 UTC on November 14, 2005 at the LIGO Livingston Observatory; the run ended at 00:00 UTC on October 1, 2007. During this run, all three LIGO detectors had displacement spectral amplitudes very near their design goals of $1.1 \times 10^{-19} \text{ m Hz}^{-1/2}$ [16] in their most sensitive frequency band near 150 Hz. (In terms of gravitational-wave strain, the H2 interferometer was roughly a factor of two less sensitive than the other two; its data were not used in this search.)

The data were acquired and digitized at a rate of 16384 Hz. Data acquisition was periodically interrupted by disturbances such as seismic transients (natural or anthropogenic), reducing the net running time of the in-

terferometers. In addition, there were 1–2 week commissioning breaks to repair equipment and address newly identified noise sources. The resulting duty factors for the interferometers were approximately 69% for H1, 77% for H2, and 57% for L1 during the first eight months. A nearby construction project degraded the L1 duty factor significantly during this early period of the S5 run. By the end of the S5 run, the cumulative duty factors had improved to 78% for H1, 79% for H2, and 66% for L1. For this search, approximately 4077 hours of H1 data and 3070 hours of L1 data were used, where each data segment used was required to contain at least 30 minutes of continuous interferometer operation.

III. SIGNAL WAVEFORMS

The general form of a gravitational-wave signal is described in terms of two orthogonal transverse polarizations defined to be “+” with waveform $h_+(t)$ and “ \times ” with waveform $h_\times(t)$, for which separate and time-dependent antenna pattern factors F_+ and F_\times apply, which depend on a polarization angle ψ [17]. For periodic gravitational waves, which in general are elliptically polarized, the individual components $h_{+,\times}$ have the form $h_+(t) = A_+ \cos \Phi(t)$ and $h_\times(t) = A_\times \sin \Phi(t)$, where A_+ and A_\times are the amplitudes of the two polarizations, and $\Phi(t)$ is the phase of the signal at the detector. For the semi-coherent method used in this search, only the instantaneous signal frequency in the detector reference frame, $2\pi f(t) = d\Phi(t)/dt$, needs to be calculated. For an isolated, precession-free, rigidly rotating neutron star the quadrupolar amplitudes A_+ and A_\times are related to wave amplitude, h_0 , by $A_+ = h_0 \frac{1+\cos^2 \iota}{2}$ and $A_\times = h_0 \cos \iota$, where ι describes the inclination angle of the star’s spin axis with respect to the line of sight. For such a star, the signal wave frequency, f , is twice the rotation frequency, f_r .

The detector reference frame frequency $f(t)$ can, to a very good approximation, be related to the frequency $\hat{f}(t)$ in the Solar System Barycenter (SSB) frame by [5] $f(t) - \hat{f}(t) \simeq \hat{f}(t) \frac{\mathbf{v}(t) \cdot \mathbf{n}}{c}$, where $\mathbf{v}(t)$ is the detector’s velocity with respect to the SSB frame, and \mathbf{n} is the unit-vector pointing from the detector toward the sky location of the source [5].

IV. ANALYSIS METHOD

The PowerFlux method used in this analysis is described in detail elsewhere [6] and is a variation upon the StackSlide method [18]. Here we summarize briefly its main features.

A strain power estimator is derived from summing measures of strain power from many short, 50%-overlap, Hann-windowed Fourier transforms (SFTs) that have been created from 30-minute intervals of calibrated strain

data. In searching a narrow frequency range (0.5 mHz spacing) for an assumed source sky location, explicit corrections are made for Doppler modulations of the apparent source frequency. These modulations are due to the Earth’s rotation and its orbital motion around the SSB, and the frequency’s time derivative, \dot{f} , intrinsic to the source. Corrections are also applied for antenna pattern modulation, assuming five different polarizations: four linear polarizations separated by $\pi/8$ in polarization angle, and circular polarization. When summing, the variability of the noise is taken into account with an SFT-dependent weight proportional to the expected inverse variance of the background noise power (see [6, 19] for detailed formulae).

The search range for initial frequency \hat{f}_0 values is 50–1100 Hz with a uniform grid spacing equal to the size of an SFT frequency bin $[1/(30 \text{ min})]$. The range of \hat{f} values searched is -5×10^{-9} – 0 Hz s^{-1} with a spacing of $5 \times 10^{-10} \text{ Hz s}^{-1}$, since isolated rotating neutron stars are generally expected to spin down with time. As discussed in our previous reports [3, 5, 6], the number of sky points that must be searched grows quadratically with the frequency \hat{f}_0 , ranging here from about five thousand at 50 Hz to about 2.4 million at 1100 Hz. The sky grid used here is isotropic and covers the entire sky.

Upper limits calculated in this method are strict frequentist limits on linear and circular polarization in small patches on the sky, with the limits quoted here being the highest limits in each 0.25-Hz band over broad regions of the sky. These are interpreted as limits on worst-case (linear polarization) and best-case (circular polarization) orientations of rotating neutron stars. Since the eight months of data analyzed here cover a large span of the Earth’s orbit, providing substantial Doppler modulation of source frequency, contamination from stationary instrumental lines is much reduced from earlier and shorter data runs. A total of only 0.6% of the search volume in sky location and spindown had to be excluded from the upper-limit analysis because of Doppler stationarity.

The primary changes in the PowerFlux algorithm used in this search concern followup of outlier candidates. (The general method for setting upper limits is identical to that used in the S4 search [6].) Here we summarize the followup method used. Single-interferometer searches are carried out separately for the H1 and L1 interferometers, leading to the upper limits on strain shown in Fig. 1 and discussed below. During determination of the maximum upper limit per sky region, per frequency band and per spin-down step, a “domain map” is constructed of local signal-to-noise ratio (SNR) maxima, with the domains ordered by maximum gridpoint SNR and clustered if close in direction and frequency. The 1000 domains with the highest maximum SNR are then re-analyzed to obtain improved estimates of the associated candidate parameters, using a modified gradient search with a matched filter to maximize SNR with respect to source frequency, spin-down, sky location, polarization angle ψ , and inclination angle ι [19]. This maximization step sam-

ples frequency and spin-down much more finely than in the initial search.

When all sky regions and all spin-downs have been searched for a given 0.25 Hz band for both H1 and L1, the search pipeline outputs are compared, and the following criteria are used to define candidates for followup analysis. The H1 and L1 candidates must each have an SNR value greater than 6.25, and they must agree in frequency to within $1/180 \text{ Hz} = 5.56 \text{ mHz}$, in spin-down to within $4 \times 10^{-10} \text{ Hz s}^{-1}$, and in sky location to within 0.14 radians. These conservative choices have been guided by simulated single-interferometer pulsar injections. Coincidence candidates within 0.1 Hz of one another are grouped together, since most candidates arise from detector spectral artifacts that become apparent upon manual investigation.

Candidates passing these criteria are subjected to a computationally intensive followup analysis that reproduces the all-sky PowerFlux search in a 0.25 Hz band around each candidate, this time using the (incoherently) combined strain powers from both interferometers. Sky maps of strain and SNR are created and examined manually for each individual interferometer and for the combined interferometers. Spectral estimates from noise decomposition are also examined to identify possible artifacts leading to the coincident outliers.

V. RESULTS

Figure 1 shows the lower of the H1 and L1 95% confidence-level upper limits on pulsar gravitational wave amplitude h_0 for worst-case and best-case pulsar orientations for different declination bands (each with different run-averaged antenna pattern sensitivity). As in the S4 analysis, narrow bands around 60-Hz power mains harmonics, along with bands characterized by non-Gaussian noise, have been excluded from the displayed limits. Numerical values for frequencies and limits displayed in these figures can be obtained separately [20]. Systematic uncertainties on these values are dominated by calibration uncertainty at the $\sim 10\%$ level.

All outliers were checked for coincidence between H1 and L1, as described above. In most cases single-interferometer spectral artifacts were readily found upon initial inspection, most of which had known instrumental or environmental sources, such as mechanical resonances (“violin modes”) of the wires supporting interferometer mirrors, and power mains harmonics of 60 Hz. Other outliers were tracked down to previously unknown electromagnetic disturbances. For six coincidence candidates, no instrumental spectral artifacts were apparent. Their 0.1-Hz bands and favored spin-down values are listed in Table I, along with the maximum SNR’s observed in H1 and L1 data.

None of these six candidates was confirmed, however, as a detection of a constant-amplitude, constant-spin-down periodic source of gravitational radiation. In each

Frequency band (Hz)	Spin-down (Hz s ⁻¹)	H1 SNR	L1 SNR
867.2	-4.3×10^{-9}	6.27	6.30
941.0	-2.0×10^{-9}	6.50	6.67
967.8	-1.5×10^{-9}	6.26	6.33
979.5	-5.0×10^{-9}	6.40	6.29
1058.6	-5.0×10^{-10}	6.83	6.38
1070.2	-3.0×10^{-10}	6.72	6.99

TABLE I: List of coincidence candidates for which no instrumental spectral artifacts were observed.

case, we found that the combined H1-L1 SNR did not increase by more than 0.6 (0.4) units over the minimum (maximum) of the single-interferometer SNR’s, with four candidates showing a *decrease* for combined SNR. To understand the expectation for a true signal, we carried out *a posteriori* software signal injections, which indicated that combined SNR should typically show an increase over minimum SNR by more than 2.0 units for a single-interferometer SNR threshold of 6.25. Hence we conservatively veto all candidates with an SNR increase less than 1 unit. In addition, manual exploration of these candidates was carried out, using larger portions of the S5 run’s data, to determine whether SNR increased with additional data, and with subsets of the the original 8-month data, to determine whether a transient astrophysical source could explain the candidate. None of these explorations proved fruitful.

We also note that multi-interferometer injections indicate that for signal frequencies above 850 Hz, the coincidence requirements in frequency and sky location could be tightened by a factor of five to 1 mHz and by a factor of seven to 0.02 radians, respectively, with only a slight reduction in efficiency for true signals. None of the candidates in Table I satisfies these tighter criteria.

In summary, we have set strict, all-sky frequentist upper limits on the strength of continuous-wave gravitational radiation of linear and circular polarization, corresponding to least favorable and most favorable pulsar orientations, respectively. Followup analysis of coincidence candidates with $\text{SNR} > 6.25$ did not yield a detection. The limits on detected strain can be translated into limits on equatorial ellipticity as small as 10^{-6} for unknown neutron stars as far away as 500 pc. This ellipticity is at the upper range thought to be sustainable by conventional neutron stars and well below the maximum sustainable (10^{-4}) by a strange quark star.

VI. ACKNOWLEDGMENTS

We thank Deepto Chakrabarty and David Kaplan for useful discussions. The authors gratefully acknowledge the support of the United States National Science Foundation for the construction and operation of the LIGO

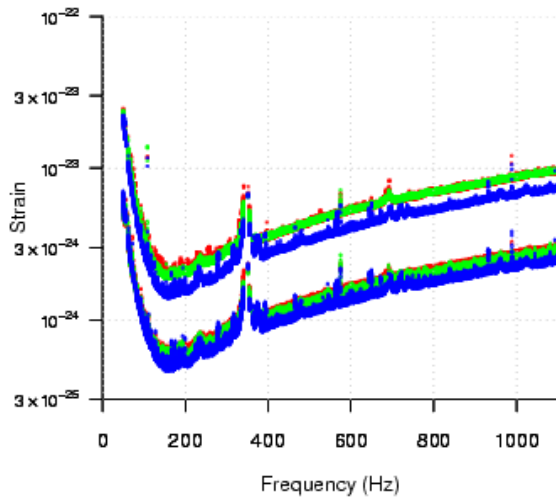


FIG. 1: Minimum (H1 or L1) upper limits (95% CL) on pulsar gravitational wave amplitude h_0 for the equatorial (red), intermediate (green), and polar (blue) declination bands for best-case (lower curves) and worst-case (upper curves) pulsar orientations. Shown are all the minimum limits for each of the 11 spin-down values from $-5 \times 10^{-9} \text{ Hz s}^{-1}$ to zero in steps of $5 \times 10^{-10} \text{ Hz s}^{-1}$.

Laboratory and the Science and Technology Facilities Council of the United Kingdom, the Max-Planck-Society, and the State of Niedersachsen/Germany for support of the construction and operation of the GEO600 detector. The authors also gratefully acknowledge the support of the research by these agencies and by the Australian Research Council, the Council of Scientific and Industrial Research of India, the Istituto Nazionale di Fisica Nucleare of Italy, the Spanish Ministerio de Educación y Ciencia, the Conselleria d'Economia Hisenda i Innovació of the Govern de les Illes Balears, the Royal Society, the Scottish Funding Council, the Scottish Universities Physics Alliance, The National Aeronautics and Space Administration, the Carnegie Trust, the Leverhulme Trust, the David and Lucile Packard Foundation, the Research Corporation, and the Alfred P. Sloan Foundation. This document has been assigned LIGO Laboratory document number LIGO-P080024-03-Z.

- [1] A. Abramovici *et al.*, Science **256**, 325 (1992).
- [2] B. Barish and R. Weiss, Phys. Today **52**, 44 (1999).
- [3] B. Abbott *et al.* (The LIGO Scientific Collaboration), Phys. Rev. D **76**, 082001 (2007).
- [4] B. Knispel and B. Allen, preprint arXiv:0804.3075 [gr-qc].
- [5] B. Abbott *et al.* (The LIGO Scientific Collaboration), Phys. Rev. D **72**, 102004 (2005).
- [6] B. Abbott *et al.* (The LIGO Scientific Collaboration), Phys. Rev. D **77**, 022001 (2008).
- [7] The Einstein@Home project is built upon the BOINC (Berkeley Open Infrastructure for Network Computing) architecture described at <http://boinc.berkeley.edu/>.
- [8] S3 results from the distributed computing project Einstein@Home can be found at <http://einstein.phys.uwm.edu/>.
- [9] B. Abbott *et al.* (The LIGO Scientific Collaboration), Phys. Rev. D (in press), preprint arXiv:0804.1747 [gr-qc].
- [10] G. Ushomirsky, C. Cutler, and L. Bildsten, Mon. Not. Roy. Astron. Soc. **319**, 902 (2000).
- [11] B. Owen, Phys. Rev. Lett. **95**, 211101 (2005).
- [12] R. Narayan, Ap. J. **319** 162 (1987).
- [13] D. Lorimer, Liv. Rev. Rel. **8**, 7 (2005).
- [14] J. M. Cordes and D. F. Chernoff, Ap. J. **505**, 315 (1998).
- [15] R. N. Manchester, G. B. Hobbs, A. Teoh and M. Hobbs, Astron. J. **129**, 1993 (2005). See also <http://www.atnf.csiro.au/research/pulsar/psrcat/>.
- [16] B. Abbott *et al.* (The LIGO Scientific Collaboration), in preparation, preprint arXiv:0711.3041 [gr-qc].
- [17] P. Jaranowski, A. Królak, and B. F. Schutz, Phys. Rev. D **58**, 063001 (1998).
- [18] P. Brady and T. Creighton, Phys. Rev. D **61**, 082001 (2000).
- [19] V. Dergachev, "Description of PowerFlux Algorithms and Implementation", LIGO technical document LIGO-T050186 (2005), available in <http://admbdsvr.ligo.caltech.edu/dcc/>
- [20] See EPAPS Document No. [number will be inserted by publisher] for numerical values of upper limits derived for the H1 and L1 interferometers in 0.25-Hz bands in the range 50-1000 Hz.